Three-Dimensional Acoustic Room Impulse Response Modeling With Frequency Dependent Reflections

Journal:	*Journal of Selected Topics in Signal Processing*
Manuscript ID:	J-STSP-SPSA-00171-2014
Manuscript Type:	Special Issue Paper
Date Submitted by the Author:	16-Jul-2014
Complete List of Authors:	Bhatta, Ambika; UMass Lowell, Electrical Engineering Thompson, Charles; UMass Lowell, ECE Chandra, Kavitha; UMass Lowell, ECE

SCHOLARONE™
Manuscripts
For Review Only

Three-Dimensional Acoustic Room Impulse Response Modeling With Frequency Dependent Reflections

Ambika Bhatta, *Student Member, IEEE,* Charles Thompson, *Senior Member, IEEE,* and Kavitha Chandra, *Senior Member, IEEE*

***Abstract*—A computational model for the three dimensional acoustic room impulse response is presented by extending the classical method of images to include frequency dependent wall impedances. The reflection coefficients are expressed as a Laplace transform and the solution to the inverse transform is developed. This result is applied to develop a computationally tractable integral for the acoustic pressure. The proposed method can be used to accurately estimate the spatial-temporal room impulse response with potential spatial audio applications.**

***Index Terms*—acoustics, impulse-response, images, complex impedance**

I. Introduction

The accurate modeling of the acoustic room impulse response serves many applications that range from the design of spaces to the reproduction of sound effects for virtual reality systems. There is a great deal of interest in ways to integrate acoustic effects of a room into the many current and emerging applications of digital audio. The identification of an accurate room impulse response model in space and time is important in spatial impulse reponse rendering [1], wherein the acoustic environment being modeled is rendered to the listener by synthesizing a multichannel impulse response, through which sound is convolved to emulate the acoustics of the desired enclosure. Of particular importance for spatial hearing is the recreation of a set of perceptual features that aid sound localization [2], [3]. These frequency dependent cues include the interaural time difference, the interaural level difference interaural coherence, monaural localization and timbral perception that depends on the spectral, temporal and spatial properties of sound. The direct sound, early arrivals and the reverberation signal of an impulse response all contribute to deciphering the perceptual cues. The estimation of these cues from measured and computed room impulse responses is an area of active research [4].

This work addresses the development of an accurate and computationally tractable image-source based model for estimating the spatio-temporal impulse response of a rectangular enclosure. An exact analysis of frequency and angular dependent boundary reflection coefficients is undertaken and spatial distribution of the channel impulse response is analyzed. The method of images and its application to problems where the reflection of spherical wave from a planar surface is a characteristic feature has been examined by numerous investigators for more than a hundred years. Early investigation by Sommerfeld [5] and Weyl [6] focused on the use of image theory in electromagnetics. Its importance in the field of acoustics was first demonstrated by Ingard [7] and Rudnick [8]. Since their initial investigations numerous investigators have embarked on the image solution [9]–[12] in differing contexts. Much of this work has focused on reflection from a single planar boundary under time-harmonic excitation. The objective of these studies was to use the solution to obtain workable as well as rigorous solutions to more complicated problems in acoustics. An exact image theory has been presented for the electric [13] and magnetic dipole [14] cases. Di and Gilbert [15] adapted the aforementioned work for the acoustic case.

Applying the image method in room acoustics allows one to replace the walls of the enclosure with point sources having varying strength and location. Thereby rendering the solution for the pressure in the room as a sum of simple sources. The amplitude of each image is chosen such that the pressure and the normal component of the particle velocity is continuous across the boundary. Using the method of images Allen and Berkley [16] estimated the pressure in a rectangular cavity with lossy walls. In their work, the image solution is used to construct a digital tapped delay line for the impulse response between source and receiver locations.

For Review Only

While their solution captures the temporal position of the arrivals of the reflected wave, the frequency and angular dependence of the reflected wave was not considered.

Suh and Nelson [17] consider a plane wave reflection coefficient from locally reacting surfaces as an approximation in their image-source model and compare modeled and measured impulse responses to evaluate the assumption of a real versus complex surface impedance. They found that for fairly absorbent surfaces, the complex impedance could have significant influence in the accuracy of the model. The influence of the phase angle of the surface impedance on binaural impulse responses is shown to effect a different human perception of reverberation compared to the zero phase angle case in [18], particularly at low absorption cases. This study also assumed locally reacting surfaces, with acoustically hard walls and floor and ceiling with complex surface impedance.

This work examines the problem of spherical wave reflections in a rectangular enclosure with the objective of determining the time-impulse response between source and observation points. The reflected pressure amplitude when incident pressure undergoes multiple reflections from six surfaces of a two layer medium forming a three dimensional cavity analogous to a closed room is determined. The approach is based on expressing the reflection coefficient in the wavenumber domain in terms of its Laplace transform in space and its application to Sommerfeld's integral for the response of a reflecting surface due to a point source. The method for inverting the spatial Laplace transform to obtain the effective reflection coefficient of the cavity for incorporation into the image-source model is described. The surfaces are considered to be globally reacting.

Section II describes the room geometry and specification of acoustical parameters Section III presents the formulation for the pressure response in terms of the three-dimensional reflection coefficient. The inverse Laplace transform (ILT) of a single reflection coefficient is derived. The method is extended to multiple reflections in Section IV and a computationally efficient model for the ILT is presented. Section V presents results for globally reacting surfaces. The effect of frequency dependent surface impedance is analyzed and a sample of the computed room impulse response is shown.

II. Problem Statement

Consider a rectangular cavity having dimensions (L_x, L_y, L_z) as shown in Fig. 1. The cavity is bounded by walls comprised of materials that have an impedance and sound speed that differs from that of the enclosed fluid. The rest density and sound speed in the cavity is taken to be constant and will be denoted by the variables ρ_0 and speed c_0 respectively. The impedance and sound speed of the material comprising each wall will be expressed by the double subscripted variables Z_{jq} and c_{jq}. The subscript $j = (x, y, z)$ denotes the axial direction of normal to the wall surface and the second subscript $q = (1, 2)$ is used to denote the wall. The index $q = 1$ is used to label the wall farthest from the origin of the q axis. Hence the wall impedances are $(Z_{x_{1,2}}, Z_{y_{1,2}}, Z_{z_{1,2}})$ and the sound speeds are $(c_{x_{1,2}}, c_{y_{1,2}}, c_{z_{1,2}})$.

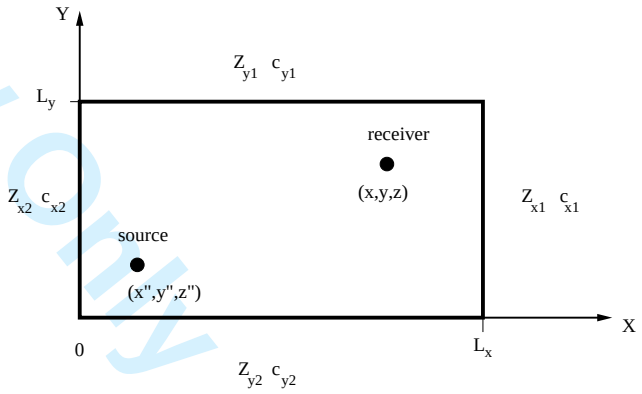

Fig. 1: Schematic of the problem geometry.

The task at hand is to determine the response at the point $\underline{x}$ that results from an impulse in time applied by point source located at $\underline{x}''$. When the spherical wave generated by the point source hits the wall surface, a portion of its energy is absorbed and the remainder is reflected. The field is taken to satisfy continuity in the pressure and in the normal component of the velocity across the wall interface. Therefore each wall is taken to behave as

For Review Only

a globally reacting medium. The process is repeated for each successive wall reflection. For plane waves the reflected wave amplitude that results from the wall interaction boundary conditions is captured by the Fresnel reflection coefficient. Adaptation of this result to spherical waves has been a subject of numerous investigations over the last one hundred years.

III. Formulation of Pressure response

The temporal Fourier transform of the pressure $P(\underline{x}, \underline{x}'', \omega)$ is given by the solution of the inhomogeneous Helmholtz equation.

$$\nabla^2 P + k_0^2 P = \delta(\underline{x} - \underline{x}'') \tag{1}$$

where the wavenumber $k_0 = \omega/c_0$, $\underline{x}$ is the observation position and $\underline{x}''$ is the source location.

When the incident pressure wave undergoes reflections from all the surfaces of the cavity, the pressure response can be estimated by superposition of reflected pressure due to each reflection. Therefore, the behavior of reflected pressure is of particular interest. The complex pressure amplitude is represented in terms of the reflection coefficient and the spatial Fourier transform of the free space Green's function as

$$P = \frac{1}{(2\pi)^3} \int_{-\infty}^{\infty} \int_{-\infty}^{\infty} \int_{-\infty}^{\infty} \sum_{\underline{n}=0} R(\hat{\underline{k}}, \underline{n}) \frac{e^{i\underline{k}\cdot(\underline{x} - \underline{x}'(\underline{n}))}}{k^2 - k_0^2} d\underline{k} \tag{2}$$

where $\underline{x}$ is the observation location and $\underline{x}'$ is the location of the $\underline{n}^{th}$ source point. The wavenumber $\underline{k} = (k_x, k_y, k_z)$ and the direction cosine of the incident angle is given by $\hat{\underline{k}} = (\frac{k_x}{k_0}, \frac{k_y}{k_0}, \frac{k_z}{k_0})$. The reflection coefficient takes the form

$$R(\hat{\underline{k}}, \underline{n}) = \prod_{j=x,y,z} R_{j1}^{N_{j1}(n_j)} R_{j2}^{N_{j2}(n_j)} \tag{3}$$

where R_{jq} for $q = 1, 2$ is the reflection coefficient from the q^{th} wall perpendicular to the j^{th} axis. The exponent N_{jq} is equal to the number of reflection from the q^{th} wall. The incident wave is recovered at $\underline{n} = 0$. Hence $N_{jq}(0) = 0$ and $\underline{x}(0) = x''$. The remainder of the terms in the sum represent reflected wave contributions.

Kuester and Chang [19] suggested an approach to simplify Eqn.(2) by rewriting R as a Laplace transform in the $\underline{p}$ domain. The reflection coefficient $R(\hat{\underline{k}}, \underline{n})$ is expressed as

$$R(\hat{\underline{k}}, \underline{n}) = \int_0^{\infty} \int_0^{\infty} \int_0^{\infty} \sum_{\underline{n}} S(\underline{p}, \underline{n}) e^{-\hat{\underline{k}}\cdot\underline{p}} d\underline{p} \tag{4}$$

given that the real part of each component of $\hat{\underline{k}}$ is greater than 0. The function $S(\underline{p}, \underline{n})$ is the inverse Laplace transform of the reflection coefficient of the cavity. Upon its substitution of Eqn. (4) into Eqn. (2) the complex pressure amplitude results in a convolution and is reduced to the following integral

$$P = \frac{1}{4\pi} \int_0^{\infty} \int_0^{\infty} \int_0^{\infty} \sum_{\underline{n}=0} S(\underline{p}, \underline{n}) \frac{e^{ik_0\psi}}{\psi} d\underline{p} \tag{5}$$

where $Im(\psi) > 0$ and

$$\psi = \sqrt{(x - x'(n_x) + i\tfrac{p_x}{k_0})^2 + (y - y'(n_y) + i\tfrac{p_y}{k_0})^2 + (z - z'(n_z) + i\tfrac{p_z}{k_0})^2} \tag{6}$$

and $S(\underline{p}, 0) = \delta(\underline{p})$. Since R is separable in $\hat{\underline{k}}$

$$S(\underline{p}, \underline{n}) = \prod_{j=x,y,z} S_j(p_j, n_j) \tag{7}$$

A. Single Reflection Inverse Laplace Transform

As discussed in the last section, the pressure response of the cavity can be estimated in terms of the inverse Laplace transform of the reflection coefficient $S(\underline{p}, \underline{n})$ which is evaluated from the plane wave reflection coefficient $R(\hat{\underline{k}}, \underline{n})$. In this section we introduce the salient features of our approach using the analysis of the reflection from a single wall. In such a case

$$S(\underline{p}, \underline{n}) = \delta(p_l)\delta(p_m) S_j(p_j) \delta_{n_j - 1} \tag{8}$$

and there are no reflections for the walls perpendicular to te l and m axis. Given that the source location is equal to $\underline{x}''$ there is single image located at x' that is the reflection about the j^{th} axis. Consider the reflection coefficient along the j^{th} axis and from wall boundary having index q. The reflection coefficient for the first reflection can be expressed in terms of normalized characteristic impedance of the medium $\hat{Z} = Z_{jq}/(\rho_0 c_0)$ and normalized speed of sound $\hat{c} = c_{jq}/c_0$.

$$R_j(\hat{k}_j) = \frac{\hat{Z}\hat{k}_j - \sqrt{1 - (1 - \hat{k}_j^2)\hat{c}^2}}{\hat{Z}\hat{k}_j + \sqrt{1 - (1 - \hat{k}_j^2)\hat{c}^2}} \tag{9}$$

Defining $\hat{\alpha}^2 = (1 - \hat{c}^2)/\hat{c}^2$ and $\hat{\gamma}^2 = (1 - \hat{c}^2)/(\hat{Z}^2 - \hat{c}^2)$ the reflection coefficient may be

For Review Only

rewritten in terms of the sum of its asymptotic value of R_j in the limit as $k_j \to \infty$ and its remainder.

$$R_j = \hat{Z} - \hat{c}(\hat{Z}+\hat{c})^{-1} + \hat{Z}\hat{c}\Big((\hat{Z}^2-\hat{c}^2)(\hat{k}_j^2-\hat{\gamma}^2)\Big)^{-1}\times \\ \times\Big[\Big(\hat{k}_j - \sqrt{\hat{k}_j^2+\hat{\alpha}^2}\Big)^2 - (\hat{Z}-\hat{c})(\hat{Z}+\hat{c})^{-1}\hat{\alpha}^2\Big] \tag{10}$$

The aforementioned expression of the reflection coefficient is inverted to obtain $S(p_j)$. The inversion contour in the $\hat{k}_j$-plane is shown in in Fig. 2. The function has two potential singularities at $\hat{k}_j = \pm\hat{\gamma}$ and only one is enclosed in the chosen contour. It is important to notice that the second term of the integrand is a function of $\sqrt{\hat{k}_j^2+\hat{\alpha}^2}$. Therefore, there will be a discontinuity of the integrand along the branch cut connecting the branch points $-i\hat{\alpha}$ and $+i\hat{\alpha}$. The local analysis of R_j about $\hat{k}_j = -\hat{\gamma}$ reveals that by virtue of a pole-zero cancellation it is analytic.

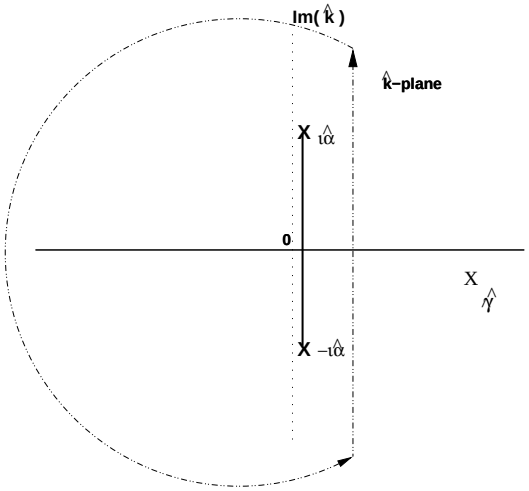

Fig. 2: Contour for inverse Laplace transform in $\hat{k}$-plane.

Hence the inverse Laplace transform of the reflection coefficient is the sum of a branch integral and a $\delta(p_j)$ function term. Using the change of variable $\hat{k}_j = i\kappa_j$ one can simplify the inverse Laplace transform of the reflection coefficient for a single reflection to

$$S_j(p_j) = (\hat{Z}-\hat{c})(\hat{Z}+\hat{c})^{-1}\delta(p_j) \; - \\ - \; 4\hat{Z}\hat{c}(\pi(\hat{Z}^2-\hat{c}^2))^{-1} \\ \int_0^{\hat{\alpha}} \kappa_i\sqrt{\hat{\alpha}^2-\kappa_i^2} \\ (\kappa_j^2+\hat{\gamma}^2)^{-1}\sin(\kappa_j p_j)d\kappa_j \tag{11}$$

IV. Multiple Reflections

When two or more boundaries are present, the incident pressure wave undergoes multiple reflections and the reflection coefficient is compounded for each wall boundary collision. This state of affairs can be expressed in terms of the product of the reflection coefficients R_{j1} and R_{j2} at the walls. The distance between the two walls is given by L_j and $n = 0$ represents the index for the source location. The image location and the evaluation of $S(p_j, n_j)$ for multiple reflections from two parallel walls will be considered next. A schematic of the geometry shown in Fig.3 for the case where $j = y$. Multiple reflections are modeled by geometrically constructed image source locations shown as ordered products of the reflection coefficients.

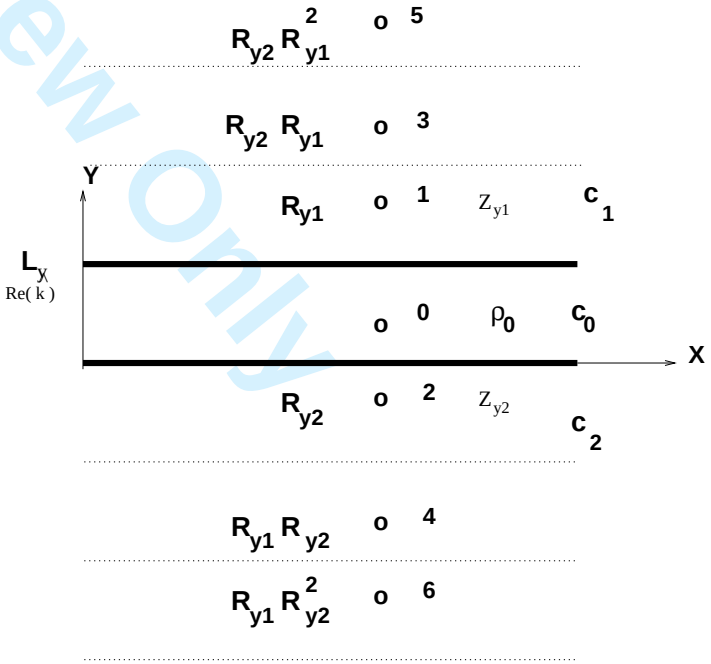

Fig. 3: Three layer medium with point source located in the middle layer.

For the case shown in Fig. 3, the location of each image is given by

$$y'(n_y) = \left\lceil \frac{\lambda(n_y)}{2} \right\rceil 2L_y + (-1)^{\lambda(n_y)} y'' \tag{12}$$

For Review Only

where $\lambda(n_y) = -(-1)^{n_y}\left\lceil \frac{n_y}{2} \right\rceil$. The reflection order is computed as

$$N_{y1}(n_y) = \lfloor \|\lambda(n_y)/2.0\| \rfloor + \|\lambda(n_y)_{mod\ 2}\| u(\lambda(n_y)) \tag{13}$$

$$N_{y2}(n_y) = \lfloor \|\lambda(n_y)/2.0\| \rfloor + \|\lambda(n_y)_{mod\ 2}\| u(-\lambda(n_y)) \tag{14}$$

where $u()$ is the Heaviside step function and $n_y = [0, \infty)$. The reflection coefficient for the n_y^{th} image is

$$R_y(\hat{k}_y, n_y) = R_{y1}^{N_{y1}(n_y)}(\hat{k}_y) R_{y2}^{N_{y2}(n_y)}(\hat{k}_y) \tag{15}$$

One can evaluate the inverse Laplace transform $S(p_y, n_y)$ from the reflection coefficient. To do so one takes the product using the using the binomial expansion recognizing that only odd multiples of the square root of the terms in the reflection coefficients will contribute to S_y. This is shown in Eq. (16). To reduce the number of computational terms of the product, the branch cuts of individual reflection coefficients is implemented to compute the inverse Laplace transform of the compound reflection coefficient. Consequently, the reflection coefficients for each wall is expressed as the sum of an analytic function A_{ym} and multi-valued term $B_{ym} f_{ym}$

$$R_y = \Big[A_{y1} + B_{y1} f_{y1}\Big]^{N_{y1}} \Big[A_{y2} + B_{y2} f_{y2}\Big]^{N_{y2}} \tag{16}$$

where

$$A_{ym} = \frac{\hat{Z}_m - \hat{c}_m}{\hat{Z}_m + \hat{c}_m} + \frac{2\hat{Z}_m \hat{c}_m}{\hat{Z}_m^2 - \hat{c}_m^2} \Big(\frac{1}{\hat{k}_y^2 - \hat{\gamma}_m^2}\Big) \Big[\hat{k}_y^2 \frac{\hat{c}_m \hat{\alpha}_m^2}{\hat{Z}_m + \hat{c}_m}\Big] \tag{17}$$

$$B_{ym} = -\frac{2\hat{Z}_m \hat{c}_m}{\hat{Z}_m^2 - \hat{c}_m^2} \Big[\frac{\hat{k}_y}{\hat{k}_y^2 - \hat{\gamma}_m^2}\Big] \tag{18}$$

$$f_{ym} = \sqrt{\hat{k}_y^2 + \hat{\alpha}_m^2} \tag{19}$$

and $\hat{Z}_m = Z_{ym}/(\rho_0 c_0)$, $\hat{c}_m = c_{ym}/c_0$, $\alpha_m = (1 - \hat{c}_m)/\hat{c}_m$ and $\hat{\gamma}_m = (1 - \hat{c}_m^2)/(\hat{Z}_m^2 - \hat{c}_m^2)$. The subscript $m = [1, 2]$ indicates the index for the wall surface. Only constant terms and odd powers of $\sqrt{\hat{k}_y^2 + \hat{\alpha}_m^2}$ need be retained for the inverse Laplace transform.

$$R_j(k_y, n_y) = a_0 + a_1 f_{y1} + a_2 f_{y2} + a_3 f_{y1} f_{y2} \tag{20}$$

The inverse Laplace transform of product of the terms that are independent of $\hat{k}_y$ will yield the delta function $\delta(p_y)$.

Therefore, the inverse Laplace transform of the reflection coefficient R_j is the sum of branch integrals

$$\begin{aligned} S_y(p_y, n_y) = S_{y0}\delta(p_y) + \oint_{-i\hat{\alpha}_1}^{+i\hat{\alpha}_1} a_1 f_{y1} e^{\kappa p} d\kappa \\ + \oint_{-i\hat{\alpha}_2}^{+i\hat{\alpha}_2} a_2 f_{y2} e^{\kappa p} d\kappa + \oint_{i\hat{\alpha}_2}^{i\hat{\alpha}_1} a_3 f_{y1} f_{y2} e^{\kappa p} d\kappa \\ + \oint_{-i\hat{\alpha}_1}^{-i\hat{\alpha}_2} f_{y1} f_{y2} e^{\kappa p} d\kappa \end{aligned} \tag{21}$$

where

$$S_{y0} = \Big(\frac{(\hat{Z}_1 - \hat{c}_1)}{(\hat{Z}_1 + \hat{c}_1)}\Big)^{N_{y1}} \Big(\frac{(\hat{Z}_2 - \hat{c}_2)}{(\hat{Z}_2 + \hat{c}_2)}\Big)^{N_{y2}} \tag{22}$$

and $\kappa = \hat{k}_y/k_0$. The contours are depicted in Fig. 4.

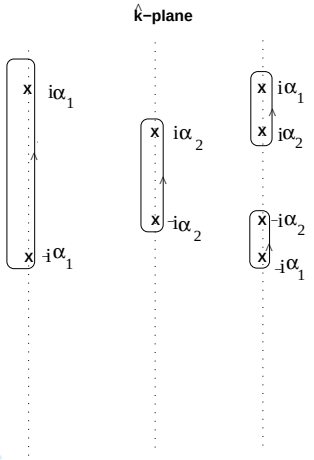

Fig. 4: Branch cuts for multiple reflection

V. Results

In the last section the image-source based pressure response of the cavity has been modeled based on an exact formulation for the inverse Laplace transform of the reflection coefficient, considering multiple reflections. In this section the impedance behavior of the walls and ceiling as a function of frequency is examined. The frequency response of the cavity when the walls have local reaction can be obtained in the limit as the speed of the sound waves in the wall is considerably smaller than that of the cavity,

For Review Only

that is $|\hat{c}| << 1$. The method presented in this work addresses the behavior when cavity walls and ceilings are globally reacting. In the results shown in Fig. 5, the ceiling and floor are chosen to have the same impedance such that $Z_{y_1} = Z_{y_2}$ and the four walls are all set to a different impedance value. The normalized boundary impedance varies as a function of frequency f and flow resistance σ and the model is derived from the experimental and analytical findings given in [20] that has been refined from the works of [21] and [22]. The flow resistance for ceiling and bottom is chosen as $\sigma = 3x10^7\ Pa.s/m^2$ and that for the walls is taken as $3x10^8\ \ Pa.s/m^2$.

The variation of the magnitude of the normalized impedance $\hat{Z}_c$ as a function of frequency is shown in Fig. 5. The change in normalized sound speed $\hat{c}$ with frequency is depicted in Fig. 6.

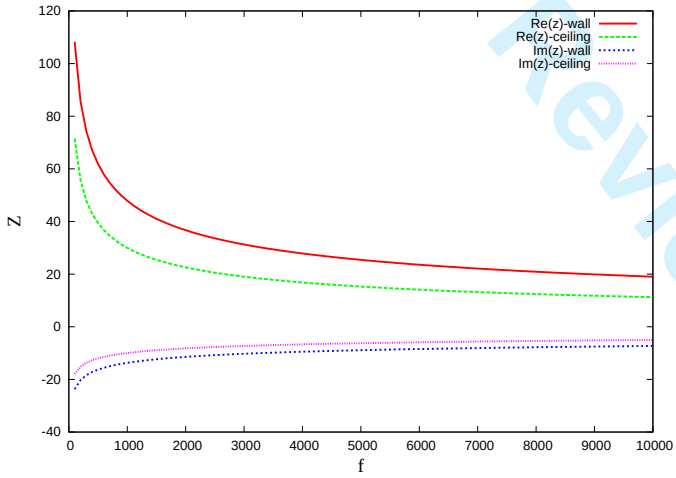

Fig. 5: Components of normalized wall and ceiling impedance for $N_t = 8192$, $\sigma_1 = 10^8$,$\sigma_2 = 3 \times 10^7$

A. *Impulse response*

The time repsonse also includes the response due to incident pressure from the source for $n = 0$. The impulse response is shown in the Fig.7 where the cavity medium is considered such that $|\hat{c}_m| < 1$ and has real impedance. The response is plotted for source location $\underline{x}'' = (1.90, 0.38, 2.28)$ meters and observation $\underline{x} = (1.14, 3.81, 1.525)$ meters with room dimensions $L = (3.05, 4.575, 3.8125)$. The sampling frequency is $f_s = 80KHz$ resulting in $N_t = 4096$ time samples. The number of images used in the computation were (n_x, n_y, n_z) : $(12, 10, 8)$

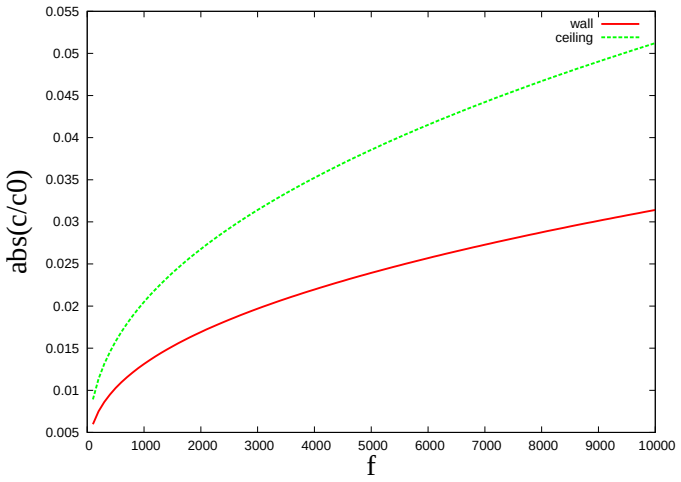

Fig. 6: Magnitude of normalized sound speed for $N_t = 8192$, $\sigma_1 = 10^8$,$\sigma_2 = 3 \times 10^7$

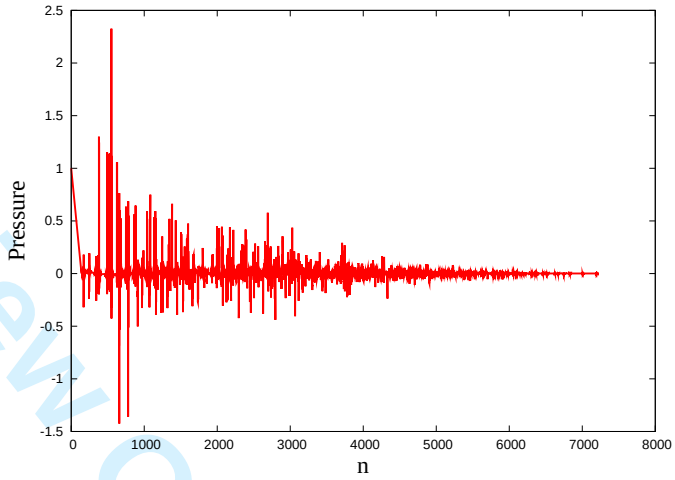

Fig. 7: Pressure response $p(\underline{x}, \underline{x}'', t)$

VI. Conclusion

A new method for computing the room impulse response using image sources has been demonstrated. The distinctive feature of the approach is the introduction of the Laplace transform method for computing the reflection coefficients that improves the convergence of the integral in the numerical method. The approach for evaluating the inverse LT of Fresnel reflection coefficients using branch integration has been shown. This method allows for frequency dependent boundary impedances, but however is limited to real values of sound speed.

VII. Acknowledgment

The authors wish to acknowledge the support of National Science Foundation grant (DGE0841394).

For Review Only

REFERENCES

[1] J. Merimaa and V. Pulkki, "Spatial impulse response rendering 1: Analysis and synthesis," *J. Audio Eng. Soc.*, vol. 53, no. 12, pp. 1115–1127, 2005.

[2] F. Baumgarte and C. Faller, "Binaural cue coding-part i: Psychoacoustic fundamentals and design principles," *IEEE Trans. Speech and Audio Proc.*, vol. 11, no. 6, pp. 509–519, 2003.

[3] C. Faller and F. Baumgarte, "Binaural cue coding-part ii: Schemes and applications," *IEEE Trans. Speech and Audio Proc.*, vol. 11, no. 6, pp. 520–531, 2003.

[4] D. Satongar, Y. W. Lam, and C. Pike, "Measurement and analysis of a spatially sampled binaural room impulse response dataset," in *21st Intl. Congress on Sound and Vibration*, 2014, pp. 1–8.

[5] A. Sommerfeld, "Propagation of waves in wireless telegraphy," *Ann. Phys.*, vol. 28, pp. 665–736, 1909.

[6] H. Weyl, "Ausbreitung elektromagnetischer wellen ber einem ebenen leiter," *Ann. Phys.*, vol. 365, pp. 481–500, 1919.

[7] U. Ingard, "On the reflection of a spherical sound wave from an infinite plane," *J. Acous. Soc. Am.*, vol. 23, pp. 329–335, 1951.

[8] I. Rudnick, "The propagation of an acoustic wave along a boundary," *J. Acoust. Soc. Am*, vol. 19, pp. 348–356, 1947.

[9] A. Wenzel, "Propagation of waves along an impedance boundary," *J. Acous. Soc. Am.*, vol. 55, pp. 956–963, 1974.

[10] S. Thomasson, "Reflection of waves from a point source by an impedance plane," *J. Acous. Soc. Am.*, vol. 59, pp. 780–785, 1976.

[11] M. Vorlander, "Simulation of the transient and steady-state sound propagation in rooms using a new combined ray-tracing/image-source algorithm," *J. Acous. Soc. Am.*, vol. 86, no. 1, pp. 172–178, 1989.

[12] D. Jarrett, E. Habets, M. Thomas, and P. Naylor, "Rigid sphere room impulse response simulation: Algorithm and applications," *J. Acous. Soc. Am.*, vol. 132, no. 3, pp. 1462–1472, 2012.

[13] V. Lindell and E. Alanen, "Exact image theory for the sommerfeld half-space problem part ii: Vertical electric dipole," *IEEE Trans. on Ant. and Prop.*, vol. AP-32, no. 8, pp. 841–847, 1984.

[14] ——, "Exact image theory for the sommerfeld half-space problem part iii: Vertical magnetic dipole," *IEEE Trans. on Ant. and Prop.*, vol. AP-32, no. 2, pp. 126–133, 1984.

[15] X. Di and K. Gilbert, "An exact laplace transform formulation for a point source above a ground surface," *J. Acous. Soc. Am.*, vol. 93, no. 2, pp. 714–720, 1993.

[16] J. B. Allen and D. B. Berkley, "Image method for efficiently simulating small-room acoustics," *J. Acoust. Soc. Am*, vol. AP-65, no. 4, pp. 943–950, 1979.

[17] J. S. Suh and P. Nelson, "Measurement of transient response of rooms and comparison with geometric acoustic models," *J. Acous. Soc. Am.*, vol. 105, no. 4, pp. 2304–2317, 1999.

[18] C. Jeong, D. Lee, , and S. Santurette, "Influence of impedance phase angle on sound pressures and reverberation times in a rectangular room," *J. Acous. Soc. Am.*, vol. 135, no. 2, pp. 712–723, 2014.

[19] E. Kuester and D. Chang, "Evaluation of sommerfeld integrals associated with dipole sources above earth," *Scientific Reports No. 43*, vol. Electromagnetics Laboratory, University of Colorado, p. 2.25, January 1979.

[20] T. Komatsu, "Improvement of delany-bazley and miki models for fibrous sund-absorbing materials," *Acoust. Sci Tech.*, vol. 29, no. 2, pp. 121–129, 2008.

[21] M. Delany and E. Bazley, "Acoustic properties of fibrous absorbent materials," *Appl. Acoustics*, vol. 3, pp. 105–116, 1970.

[22] Y. Miki, "Acoustical properties of porous materials: modification of delany-bazley models," *J. Acous. Soc. Jpn.*, vol. 11, pp. 19–24, 1990.

For Review Only